NAPETOSTNO ODVISNO RAZMIKANJE PESKA UPOŠTEVAJOČ DROBLJENJE ZRN

Fangwei Yu
Chinese Academy of Sciences,
Institute of Mountain Hazards and Environment
Chengdu 610041, Kitajska

The University of Tokyo,
Department of Civil Engineering
Tokio 113-8656, Japonska

E-pošta: fwyuui@gmail.com

Ključne besede

kot razmikanja; strižni kot; drobljenje delcev; pesek; triosni preizkus

Izvleček

V članku je predstavljeno napetostno odvisno razmikanje peska z upoštevanjem drobljenja zrn. Za ta namen je bil izveden niz dreniranih triosnih preizkusov na kremenovem pesku številka 5 in predhodno zdrobljenih peskih, ki so bili pridobljeni z več dreniranimi triosnimi preizkusi na kremenovem pesku številka 5 pri 3 MPa bočnega tlaka, s čimer je ponazorjeno striženje peska pri visokih tlakih, to pa ima za posledico drobljenje delcev. Za podani začetni količnik por je bilo ugotovljeno, da ima drobljenje delcev za posledico zmanjšanje napetostno odvisnega razmikanja peska, kar se kaže bodisi kot kontrakcijsko obnašanje ali kot zmanjšanje maksimalne vrednosti kota razmikanja in s tem zmanjšanje dodatnega strižnega kota (razlika med vrhunsko vrednostjo strižnega kota ter strižnim kotom pri kritičnem stanju). Z uvedbo koncepta količnika por skeleta pri obravnavanju drobljenja zrn je predlagan linearen odnos za napetostno odvisno razmikanje v obliki zveze med maksimalnim kotom razmikanja, dodatnim strižnim kotom in vrhnjo vrednostjo količnika por skeleta v pol-logarimični ravnini. Ta zveza je nato razširjena na mobilizirano napetostno-deformacijsko stanje. Dobljena enačba napetostno odvisnega razmikanja, ki vključuje drobljenje zrn, je uporabna za oceno vpliva drobljenja zrn na napetostno odvisno razmikanje peska.

STRESS-DILATANCY BEHAVIOR OF SAND INCORPORATING PARTICLE BREAKAGE

Fangwei Yu
Chinese Academy of Sciences,
Institute of Mountain Hazards and Environment
Chengdu 610041, China

The University of Tokyo,
Department of Civil Engineering
Tokyo 113-8656, Japan

E-mail: fwyuui@gmail.com

Keywords

dilatancy angle; friction angle; particle breakage; sand; triaxial tests

Abstract

This paper presents the stress-dilatancy behavior of sand incorporating particle breakage. A series of the drained triaxial tests were conducted on the Silica sand No.5 and the pre-crushed sands that were produced by several drained triaxial tests on Silica sand No.5 under 3MPa confining pressure in simulating the high-pressure shear process to result in particle breakage, to investigate the stress-dilatancy behavior of sand incorporating particle breakage. For a given initial void ratio, particle breakage was found to result in deterioration of the stress-dilatancy behavior in the impairment of the dilatancy of sand to become more contractive with a reduction in the maximum dilatancy angle and the excess friction angle (the difference between the peak-state friction angle and the critical-state friction angle). By introducing the concept of the skeleton void ratio in considering particle breakage, a linear stress-dilatancy relationship between the maximum dilatancy angle-over-the excess friction angle and peak-state skeleton void ratio was proposed in semi-logarithmic plane and popularized to the mobilized stress-stain state as a stress-dilatancy equation pertaining to particle breakage, which would be useful in assessing the evolution of the stress-dilatancy behavior of sand during particle breakage.

1 INTRODUCTION

Since the dilatacny phenomenon of granular materials was firstly mentioned by Reynolds (1885) [17], the dilatancy behavior of soil plays a very significant role in soil behavior, e.g., stress-dilatancy behavior of soil (e.g., [4], [5], [18], [27]), and stress-dilatancy behavior of soil in relation to particle breakage or fine content (e.g., [6], [7], [19], [22], [25], [28], [29], [30]). For a given initial void ratio, the increase of the particle breakage or the non-plastic fines was found to lead to a decrease of the dilatancy behavior of soil in a great deal of previous studies (e.g., [2], [3], [14], [16], [20], [21], [28], [29], [30]). Also, particle breakage or non-plastic fines revealed a great influence on the critical state behavior of the soil: critical state line, critical-state stress and critical-state friction angle (e.g., [2], [16], [21], [26], [28], [29], [30]). In addition, the intergranular void ratio has been used to represent the behavior of the mixed soils (e.g., [13], [15], [19], [21]). The excess friction angle (the difference between peak-state friction angle and critical-state friction angle) was widely employed in relation to the peak-state dilatancy rate for representing the stress-dilatancy behavior of soils (e.g., [3], [4], [23], [27], [29]). However, a question arises as to what role particle breakage plays in the stress-dilatancy behavior of soil, especially for the stress-dilatancy equation of soil, which has not been fully studied yet.

In this paper, with the main attempt being to establish a stress-dilatancy equation incoporating particle breakage, a series of the drained triaxial test were conducted to investigate the influence of particle breakage on the stress-dilatancy behavior of the pre-crushed sands that were produced by several triaxial tests on Silica sand No.5 under 3MPa confining pressure in simulating the high-pressure shear process to result in particle breakage. The excess friction angle, dilatancy angle and the relation of the maximum dilatancy angle over the excess friction angle of the pre-crushed sands were discussed in detail in view of particle breakage. By introducing the skeleton void ratio in considering the influence of particle breakage, a linear relation between the maximum dilatancy angle-over-the excess friction angle and the peak-state skeleton void ratio was proposed in semi-logarithmic plane and extended to the mobilized stress-stain state as a stress-dilatancy equation for particle breakage.

2 LABORATARY EXPERIMENTS

2.1 Materials and methods

As a kind of natural silica sand, Silica sand No.5 from the Seto area of Aichi prefecture, Japan-which has some of the purest sands in Japan-was tested by triaxial tests in this paper with its physical properties in Table 1 and its original grain size distribution curve in Figure 1 (JGS 0131-2009, 2009 [9]; JGS 0161-2009, 2009 [10]). Silica sand No.5 is classified as a poorly graded sand (SP) according to the Unified Soil Classification System (ASTM D2487-11, 2011 [1]).

For consistency with the previous studies [28, 29, 30], a series of Consolidated-Drained (CD) triaxial tests were conducted on Silica sand No.5 and its pre-crushed sands using a strain-controlled high-pressure triaxial apparatus with maximum 3MPa confining pressure (JGS 0524-2009, 2009 [12]). All the specimens in diameter 75mm and height 160mm were prepared by air pluviation into a mound with a 1-mm-thick membrane in eight layers with the necessary tamping to reach the designated void ratio (JGS 0520-2009, 2009 [11]). To prevent the membrane from being pierced by sharp edges of soil particles and minimizing the membrane penetration under high effective stress, a 1-mm-thick membrane was employed for all the tests. All the triaxial tests were conducted on saturated specimens with Skempton's B value over 0.98 using the de-aired water to flush the specimens under around -100kPa vacuum.

After the shearing of each test, the whole material of the specimen was dried in an oven and later mixed uniformly, and then laid open uniformly as a thin cylinderical shape on a large tray, which was divided into four sectors uniformly. The diagonal two of them were removed until around 200g left by repeating this method, with the aim to have around 200g uniform material of specimen to sieve. Hereafter, the around 200g of specimen was employed for sieve analysis to obtain the grain size distribution curve (JGS 0131-2009, 2009 [9]).

Table 1. Physical properties of Silica sand No.5.

Property	Silica sand No.5
Specific gravity, G_s	2.761
Minimum void ratio, e_{min}	0.766
Maximum void ratio, e_{max}	1.215
Fine content, F_c	0.02%
Coefficient of uniformity, C_u	1.647
Coefficient of curvature, C_c	0.378

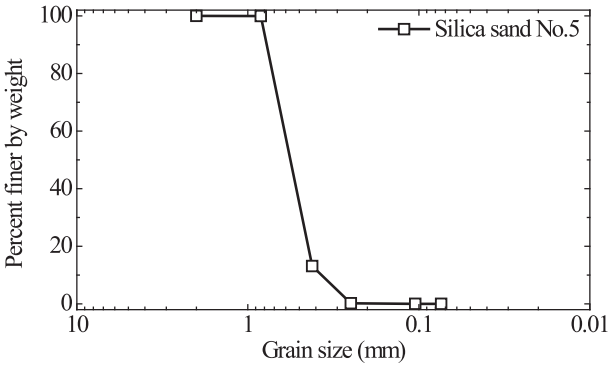

Figure 1. Original grain size distribution curve of silica sand No.5.

2.2 Quantification of particle breakage

In this paper, the Relative Breakage (B_r) [8] was introduced to assess the extent of particle breakage, where the area between initial grain size distribution curve and the grain size distribution curve after loading can be regarded as the total breakage B_t, and the area between initial grain size distribution curve and the vertical line of 0.075mm sieve size can be regarded as the breakage potential B_p. The relative breakage B_r is defined as a ratio of the total breakage B_t over the breakage potential B_p as illustrated in Figure 2.

2.3 Test results

As shown in Figure 3, several drained triaxial tests were sheared under 3MPa to the designated axial strain levels from 0% to 50% using a 10% increment for producing the crushed sands with progressively increased extent of particle breakage, which can be called the pre-crushed sands shown in Figure 4. Note that the original sand

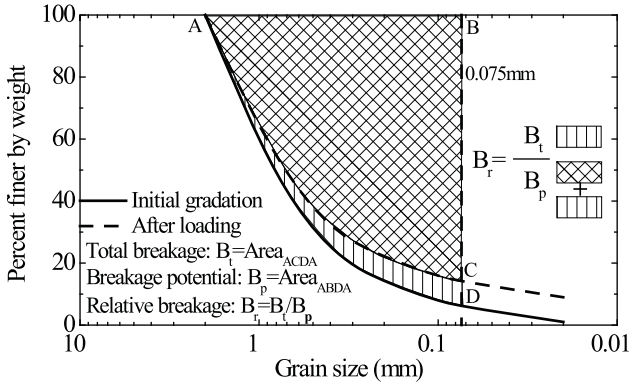

Figure 2. Definition of relative breakage (Hardin, 1985).

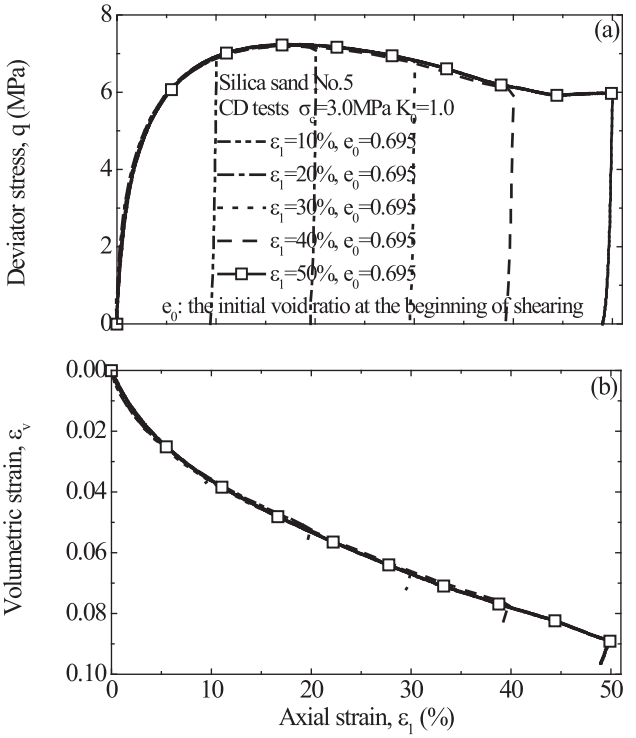

Figure 3. Drained shear tests for producing the pre-crushed sands.

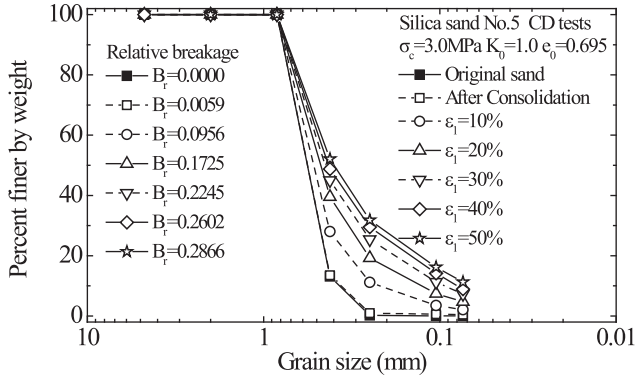

Figure 4. Grain size distribution curves of the pre-crushed sands.

can be regarded as a kind of pre-crushed sand with B_r=0.0000, and the original sand and pre-crushed sands are hereafter called the pre-crushed sands by a general designation. For investigating the influence of particle breakage on the stress-dilatancy behavior of sand, the

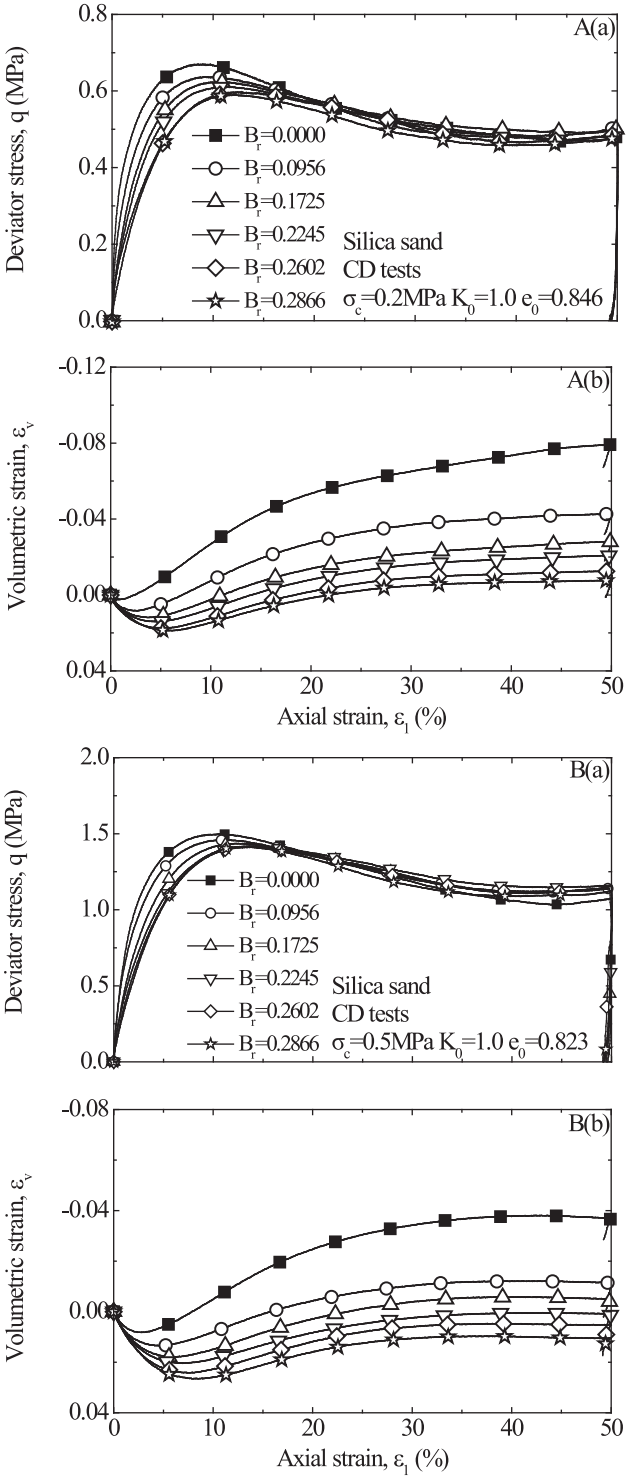

Figure 5. Drained shear results on the pre-crushed sands: (A) under 0.2MPa; (B) under 0.5MPa.

pre-crushed sands were re-employed to constitute the new specimens, which would reach the same initial void ratio after the isotropically drained consolidation and then would be re-sheared to reach the critical states under 0.2MPa and 0.5MPa confining pressures, respectively, as shown in Figure 5. Herein, the 0.2MPa and 0.5MPa, as the relatively low confining pressures were employed in the drained triaxial shear for trying not to crush the pre-crushed sands any more in clearly detecting the influence of particle breakage on the shear behavior of the pre-crushed sands. Note that the particle breakage has a significant influence on the soil behavior, e.g., for a given initial void ratio, particle breakage results in a deterioration of stress-strain behavior in the impairment of dilatancy of sand to become more contractive.

3 DISCUSSION

3.1 Angles of shearing and dilatancy

The shear strength and dilatancy of soil has a significant influence on soil behavior. The mobilized angles of shearing and dilatancy of soil are defined and given respectively by

$$\sin\varphi_m = \left[\frac{\sigma_1'/\sigma_3' - 1}{\sigma_1'/\sigma_3' + 1}\right]_m \qquad (1)$$

$$\sin\psi_m = \left[-\frac{d\varepsilon_v}{d\gamma_{13}}\right]_m \qquad (2)$$

where φ_m is the mobilized angle of shearing, ψ_m is the mobilized angle of dilatancy, σ_1'/σ_3' is the mobilized effective principal stress ratio, $d\varepsilon_v$ is the volumetric strain increment and $d\gamma_{13}$ is the maximum shear strain increment that can be calculated by $d\gamma_{13}=2d\varepsilon_1-d\varepsilon_v$ ($d\varepsilon_1$ is the axial strain increment) for the plain strain shear and traditional triaxial shear (e.g., [4], [19]).

By introducing the peak-state and critical-state stresses and strains to equations (1) and (2), the angles of shearing and dilatancy in peak state and critical state would be obtained, as represented by φ_{ps} and ψ_{ps} for peak-state friction angle and peak-state dilatancy angle, respectively, and by φ_{cs} and ψ_{cs} for critical-state friction angle and critical-state dilatancy angle, respectively.

The excess friction angle ([23], [27], [29]) is defined as

$$\varphi_{excess} = \varphi_{ps} - \varphi_{cs} \qquad (3)$$

And, corresponding to the concept of the excess friction angle, the excess dilatancy angle ψ_{excess} can be also be defined by

$$\psi_{excess} = \psi_{ps} - \psi_{cs} \qquad (4)$$

In addition, the maximum dilatancy rate of soil is widely accepted to be associated with the peak state of shear (e.g., [4]), which means that the peak-state dilatancy angle ψ_{ps} could be treated as being equal to the maximum dilatancy angle $\psi_{\max}$, i.e. $\psi_{ps}=\psi_{\max}$. And the critical-state dilatancy angle would be equal to zero, i.e. $\psi_{cs}=0$, according to the concept of critical state.

Therefore, the equation (4) gives

$$\psi_{excess} = \psi_{ps} = \psi_{\max} \qquad (5)$$

Figure 6 shows that the excess friction angles decrease approximately in up concavity to converge with increasing particle breakage. As shown in Figure 7, the maximum dilatancy angles are found to decrease gradually in slightly up concavity with increasing particle breakage. It is evident to image that the excess friction angle and maximum dilatancy angle should finally converge to a constant with increasing particle breakage to the limit particle breakage, i.e., the ratio of maximum dilatancy

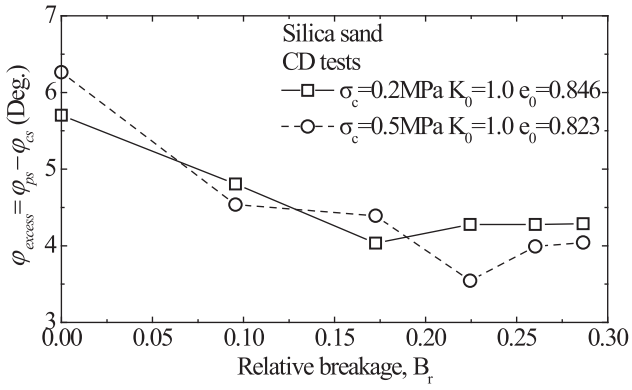

Figure 6. Evolution of the excess friction angle against relative breakage.

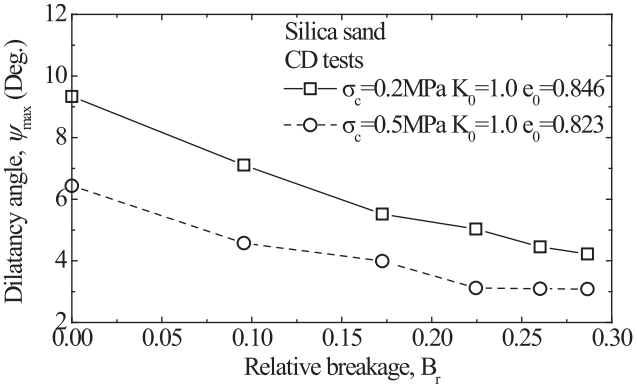

Figure 7. Evolution of the maximum dilatancy angle against relative breakage.

angle over the excess friction angle should finally converge gradually to a constant with increasing particle breakage to the limit particle breakage. Figure 8 shows the evolution of the maximum dilatancy angle-over-the excess friction angle (or the excess dilatancy angle-over-the excess friction angle) against the relative breakage, i.e., in detail, the ratio of the maximum dilatancy angle-over-the excess friction angle decreases gradually in down concavity.

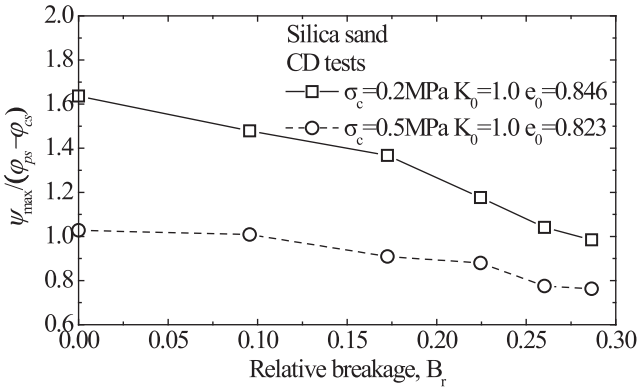

Figure 8. Evolution of the maximum dilatancy angle-over-the excess friction angle against relative breakage.

3.2 Microstructure framework for the pre-crushed sands

The increased fine content that squeezed into voids among the sand particles would result in the reduction of the maximum void ratio and minimum void ratio, which represents a reduction in the void ratios (e.g., [14], [19], [21]). For a given overall void ratio of soil with almost all the fines in voids, in the microstructure framework of granular mix, the skeleton void ratio e_{skfc} (e.g., [13], [19], [21]) can be approximately in consideration of the composite mix of coarse and fine grain skeletons as if the fines were voids, as defined by

$$e_{skfc} = \frac{1+e}{1-f_c} - 1 \qquad (6)$$

where e is the void ratio and f_c is the fine content.

As shown in Figure 3, the pre-crushed sands were produced by the progressive triaxial shear on poorly graded silica sand No.5 with very few initial fine content and lots of voids among the soil particles. With the progressive triaxial shear, the particle breakage in pre-crushed sands were regarded as being progressive, and the fine content in the pre-crushed sands can be assumed to be squeezed into the voids in the sand skeleton as if the fines were voids in being same as the concept of the skeleton void ratio. Consequently, for the pre-crushed sands with progressive particle breakage, the skeleton void ratio was introduced and redefined as the relative breakage skeleton void ratio in replacing the fine content f_c by the relative breakage B_r for considering particle breakage, as represented by

$$e_{sk} = \frac{1+e}{1-B_r} - 1 \qquad (7)$$

where e is the void ratio of original sand and B_r is the relative breakage ($0 \le B_r < 1$ corresponding to $e \le e_{sk}$). The e_{sk} with (B_r=0) is equal to the void ratio of original sand (B_r=0), and the e_{sk} is to increase monotonically with increasing particle breakage (B_r) which reveals that e_{sk} can interpret the influence of particle breakage produced by the original sand on the void ratio.

3.3 Stress-dilatancy behavior incorporating particle breakage

As illustrated in Figure 9 and Figure 10, both the excess friction angle and the maximum dilatancy angle decrease in up concavity when increasing the peak-state skeleton void ratio, which are consistent with the findings found in Figure 6 and Figure 7. As mentioned above, the ratio of maximum dilatancy angle over the

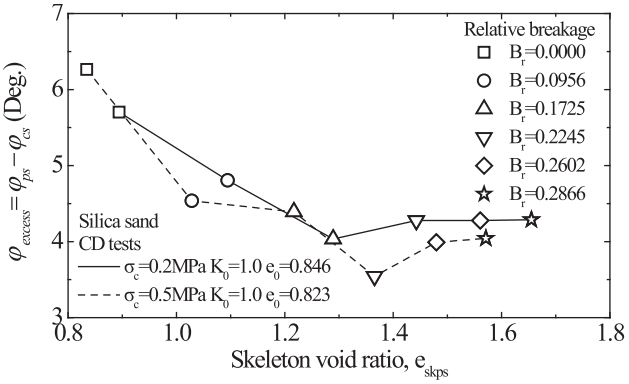

Figure 9. Evolution of the excess friction angle against peak-state skeleton void ratio.

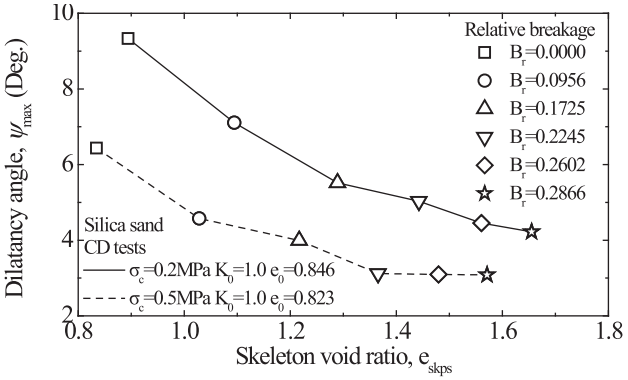

Figure 10. Evolution of the maximum dilatancy angle against peak-state skeleton void ratio.

excess friction angle should finally converge gradually to a constant with increasing particle breakage to the limit particle breakage. Meanwhile, in view of the mapping from B_r in domain [0,1) to e_{sk} in domain [e,∞), a linear relation of the maximum dilatancy angle-over-the excess friction angle and the peak-state skeleton void ratio can be drawn in semi-logarithmic plane, as displayed in Figure 11. It is also shown in Figure 11 that the different confining pressures have a significant influence on this stress-dilatancy relation, i.e., lower stress (0.2MPa) results in a much sharper decrease than the relative higher stress (0.5MPa).

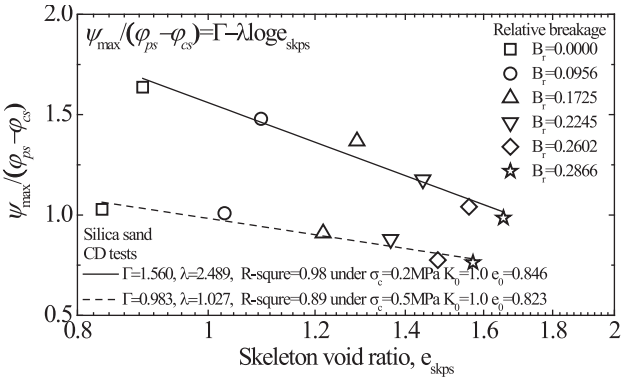

Figure 11. Evolution of the maximum dilatancy angle-over-the excess friction angle against peak-state skeleton void ratio.

As shown in Figure 11, the linear correlation between $\psi_{max}/\varphi_{excess}$ and e_{sk} can be represented by

$$\psi_{max}/\varphi_{excess}=\Gamma-\lambda\log e_{skps} \qquad (8)$$

where Γ and λ are the model parameters. By substituting equations (2), (3) and (7) into equation (8), equation (8) can be rearranged by

$$\left[-\frac{d\varepsilon_v}{d\gamma_{13}}\right]_{max}=\sin\left\{\left[\Gamma-\lambda\left(\log\frac{1+e_{ps}}{1-B_r}-1\right)\right]\left(\varphi_{ps}-\varphi_{cs}\right)\right\} \qquad (9)$$

The relation, i.e., equation (9), can be extended into the whole shear stage in replacing the peak-state variables: maximum dilatancy angle, peak-state friction angle and peak-state void ratio by the mobilized variables during shear [24], as rewritten by

$$\left[-\frac{d\varepsilon_v}{d\gamma_{13}}\right]_{m}=\sin\left\{\left[\Gamma-\lambda\left(\log\frac{1+e}{1-B_r}-1\right)\right]\left(\varphi_m-\varphi_{cs}\right)\right\} \qquad (10)$$

where e is the void ratio of the original sand, φ_m=arcsin[(σ_1'/σ_3' -1)/(σ_1'/σ_3'+1)]$_m$ is the mobilized friction angle. Equation (10) as a stress-dilatancy relation in relation to particle breakage (B_r) can be employed for application in assessing the evolution of the stress-dilatancy behavior of sand in considering the particle breakage.

4 CONCLUSIONS

A series of the drained triaxial tests were conducted on the Silica sand No.5 and the pre-crushed sands that were produced by several drained triaxial tests on Silica sand No.5 under 3MPa confining pressure in simulating the high-pressure shear process to result in particle breakage, to investigate the stress-dilatancy behavior of sand incorporating particle breakage. The major findings can be summarized as what follows:

a) For a given initial void ratio, particle breakage had a significant influence on the stress-dilatancy behavior, in impairment of dilatancy of sand to become more contractive. The skeleton void ratio was introduced in replacing the fine content by relative breakage to consider the influence of the particle breakage.
b) A linear relation between $\psi_{max}/(\varphi_{ps}-\varphi_{cs})$ and e_{skps} was proposed in $\psi_{max}/(\varphi_{ps}-\varphi_{cs})$ - log e_{skps} plane and popularized to the mobilized stress-strain state for establishing a new stress-dilatancy equation pertaining to particle breakage in assessing the stress-dilatancy behavior subjected to particle breakage.

Acknowledgements

This work was supported by the Chinese Academy of Sciences (CAS) "Light of West China" Program (Grant No.Y6R2250250), the Key Research Program of Frontier Sciences, CAS (Grant No.QYZDB-SSW-DQC010), the National Basic Research Program of China (973 Program) (Grant No.2013CB733201), the One-Hundred Talents Program of Chinese Academy of Sciences (Lijun Su) and the China Scholarship Council (Grant No.2011671035). A special acknowledgement should be expressed to Professor Ikuo Towhata for his invaluable assistance in the performance of the tests in this paper in the Geotechnical Engineering Laboratory of The University of Tokyo, Japan.

REFERENCES

[1] ASTM D2487-11, 2011. Standard Practice for Classification of Soils for Engineering Purposes (Unified Soil Classification System). ASTM International, West Conshohocken, PA. DOI:10.1520/D2487-11.
[2] Bandini, V., Coop, M.R. 2011. The influence of particle breakage on the location of the critical state line of sands. Soils and Foundations 51, 4, 591-600. DOI:10.3208/sandf.51.591.
[3] Been, K., Jefferies, M.G. 1985. A state parameter for sands. Geotechnique 35, 2, 99-112. DOI:10.1680/geot.1985.35.2.99.

[4] Bolton, M.D. 1986. The strength and dilatancy of sands. Geotechnique 36, 1, 65-78. DOI:10.1680/geot.1986.36.1.65.

[5] De Silva, L.I.N., Koseki, J., Wahyudi, S., Sato, T. 2014. Stress–dilatancy relationships of sand in the simulation of volumetric behavior during cyclic torsional shear loadings. Soils and Foundations 54, 4, 845-858. DOI:10.1016/j.sandf.2014.06.015.

[6] Hamidi, A., Alizadeh, S.M., Soleimani, M. 2009. Effect of particle crushing on shear strength and dilation characteristics of sand-gravel mixtures. International Journal of Civil Engineering 7, 61-72. DOI:10.3328/IJGE.2009.03.01.29-38.

[7] Hamidi, A., Soleimani, M. 2012. Shear strength-dilation relation in cemented gravely sands. International Journal of Geotechnical Engineering 6, 415-425. DOI:10.1179/1939787913Y.0000000026.

[8] Hardin, B.O. 1985. Crushing of soil particles. Journal of Geotechnical Engineering 111, 10, 1177-1192. DOI:10.1061/(ASCE)0733-9410(1985)111:10(1177).

[9] JGS 0131-2009. 2009. Laboratory Testing Standards of Geomaterials: Tests for physical properties-Test Method for Particle Size Distribution of Soils of Soils. The Japanese Geotechnical Society, Tokyo, Japan.

[10] JGS 0161-2009. 2009. Laboratory Testing Standards of Geomaterials: Tests for physical properties-Test Method for Minimum and Maximum Densities of Sands. The Japanese Geotechnical Society, Tokyo, Japan.

[11] JGS 0520-2009. 2009. Laboratory Testing Standards of Geomaterials:Tests for Mechanical Properties-Preparation of Soil Specimens for Triaxial Tests. The Japanese Geotechnical Society, Tokyo, Japan.

[12] JGS 0524-2009. 2009. Laboratory Testing Standards of Geomaterials: Tests for Mechanical Properties- Method for Consolidated Drained Triaxial Compression Test on Soils. The Japanese Geotechnical Society, Tokyo, Japan.

[13] Kuerbis, R.H. 1989. Effect of gradation and fines content on the undrained response of sand. Master thesis, The University of British Columbia. DOI:10.14288/1.0062832.

[14] Lade, P.V., Yamamuro, J.A. 1997. Effects of nonplastic fines on static liquefaction of sands. Canadian Geotechnical Journal 34, 6, 918-928. DOI:10.1139/t97-052.

[15] Murthy, T.G., Loukidis, D., Carraro, J.A.H., Prezzi, M., Salgado, R. 2007. Undrained monotonic response of clean and silty sands. Geotechnique 57, 3, 273-288. DOI:10.1680/geot.2007.57.3.273.

[16] Ni, Q., Tan, T.S., Desari, G.R., Hight, D.W. 2004. Contribution of fines to the compressive strength of mixed soils. Geotechnique 54, 9, 561-569. DOI:10.1680/geot.2004.54.9.561.

[17] Reynolds, O. 1885. On the dilatancy of media composed of rigid particles in contact with experimental illustrations. Philosophical Magazine 5, 20, 469-481. DOI:10.1080/14786448508627791.

[18] Rowe, P.W. 1962. The stress-dilatancy relation for static equilibrium of an assembly of particles in contact. Proceedings of the Royal Society, London, A269:500-527. DOI:10.1098/rspa.1962.0193.

[19] Salgado, R., Bandini, P., Karim, A. 2000. Shear strength and stiffness of silty sand. Journal of Geotechnical and Geoenvironmental Engineering 126, 5, 451-462. DOI:10.1061/(ASCE)1090-0241(2000)126:5(451).

[20] Thevanayagam, S. 1998. Effect of fines and confining stress on undrained shear strength of silty sands. Journal of Geotechnical and Geoenvironmental Engineering 124, 6, 479-491. DOI:10.1061/(ASCE)1090-0241(1998)124:6(479).

[21] Thevanayagam, S., Shenthan, T., Mohan, S., Liang, J. 2002. Undrained Fragility of clean sands, silty sands and sandy silts. Journal of Geotechnical and Geoenvironmental Engineering 128, 10, 849-859. DOI:10.1061/(ASCE)1090-0241(2002)128:10(849).

[22] Ueng, Tzou-shin, Chen, Tse-jen. 2000. Energy aspects of particle breakage in drained shear of sands. Geotechnique 50, 1, 65-72. DOI:10.1680/geot.2000.50.1.65.

[23] Vaid, Y.P., Sasitharan, S. 1992. The strength and dilatancy of sand. Canadian Geotechnical Journal 29, 3, 522-526. DOI:10.1139/t92-058.

[24] Wang, R.G., Guo, P.J. 1998. A simple constitutive model for granular soils: modified stress-dilatancy approach. Computers and Geotechnics 22, 2, 109-133. DOI:10.1016/S0266-352X(98)00004-4.

[25] Xiao, Y., Liu, H., Chen, Y., Chu, J. 2014. Strength and dilatancy of silty sand. Journal of Geotechnical and Geoenvironmental Engineering 140, 7, 06014007. DOI:10.1061/(ASCE)GT.1943-5606.0001136.

[26] Xiao, Y., Liu, H.L., Ding, X.M., Chen, Y.M., Jiang, J.S., Zhang, W.G. 2016. Influence of particle breakage on critical state line of rockfill material. International Journal of Geomechanics 16, 1, 04015031. DOI: 10.1061/(ASCE)GM.1943-5622.0000538.

[27] Xiao, Y., Liu, H.L., Sun, Y.F., Liu, H., Chen, Y.M. 2015. Stress-dilatancy behaviors of coarse granular soils in three-dimensional stress space. Engineering Geology 195, 104-110. DOI:10.1016/j.enggeo.2015.05.029.

[28] Yu, F.W. 2017a. Particle breakage and the critical state of sands. Geotechnique DOI:10.1680/jgeot.15.P.250. (Published online).

[29] Yu, F.W. 2017b. Particle breakage and the drained shear behavior of sands. International Journal of Geomechanics 17, 8, 04017041. DOI:10.1061/(ASCE)GM.1943-5622.0000919. (In press).

[30] Yu, F.W., Su, L.J. 2016. Particle breakage and the mobilized drained shear strengths of sand. Journal of Mountain Science 13, 8, 1481-1488. DOI:10.1007/s11629-016-3870-1.